



## Review

## Diamond semiconductor technology for RF device applications

Yasar Gurbuz<sup>a,\*</sup>, Onur Esame<sup>a</sup>, Ibrahim Tekin<sup>a</sup>, Weng P. Kang<sup>b</sup>, Jimmy L. Davidson<sup>b</sup><sup>a</sup> Sabanci University, Faculty of Engineering and Natural Sciences, Orhanli, Tuzla, 34956 Istanbul, Turkey<sup>b</sup> Vanderbilt University, Department of Engineering and Computer Engineering, Nashville, TN 37235, USA

Received 27 August 2004; accepted 10 April 2005

Available online 8 June 2005

The review of this paper was arranged by Prof. S. Cristoloveanu

**Abstract**

This paper presents a comprehensive review of diamond electronics from the RF perspective. Our aim was to find and present the potential, limitations and current status of diamond semiconductor devices as well as to investigate its suitability for RF device applications. While doing this, we briefly analysed the physics and chemistry of CVD diamond process for a better understanding of the reasons for the technological challenges of diamond material. This leads to Figure of Merit definitions which forms the basis for a technology choice in an RF device/system (such as transceiver or receiver) structure. Based on our literature survey, we concluded that, despite the technological challenges and few mentioned examples, diamond can seriously be considered as a base material for RF electronics, especially RF power circuits, where the important parameters are high speed, high power density, efficient thermal management and low signal loss in high power/frequencies. Simulation and experimental results are highly regarded for the surface acoustic wave (SAW) and field emission (FE) devices which already occupies space in the RF market and are likely to replace their conventional counterparts. Field effect transistors (FETs) are the most promising active devices and extremely high power densities are extracted (up to 30 W/mm). By the surface channel FET approach 81 GHz operation is developed. Bipolar devices are also promising if the deep doping problem can be solved for operation at room temperature. Pressure, thermal, chemical and acceleration sensors have already been demonstrated using micromachining/MEMS approach, but need more experimental results to better exploit thermal, physical/chemical and electronic properties of diamond.

© 2005 Elsevier Ltd. All rights reserved.

**Keywords:** Diamond; RF device; Chemical vapour deposition (CVD)**Contents**

1. Introduction . . . . .	1056
2. Material issues and technological challenges. . . . .	1057
3. Diamond RF electronics. . . . .	1059
3.1. Diamond based diodes. . . . .	1059
3.2. Diamond BJT . . . . .	1061
3.3. Diamond FETs . . . . .	1062
3.3.1. Boron $\delta$ -doped channel FETs . . . . .	1062
3.3.2. Surface channel FETs . . . . .	1063
3.4. Diamond RF MEMS. . . . .	1065

\* Corresponding author. Tel.: +90 216 4839533; fax: +90 216 4839550.

E-mail address: [yasar@sabanciuniv.edu](mailto:yasar@sabanciuniv.edu) (Y. Gurbuz).

3.5.	Diamond-based surface acoustic wave (SAW) devices . . . . .	1066
3.6.	Diamond field emission devices . . . . .	1066
3.7.	Thermal management with diamond devices . . . . .	1067
3.8.	Performance summary of diamond RF devices . . . . .	1069
4.	Summary and future trends . . . . .	1069
	Acknowledgements . . . . .	1070
	References . . . . .	1070

## 1. Introduction

Diamond, known for more than 200 years, has been a dream for the device engineers due to its unique material properties. It was identified as carbon in 1796, but synthesized in 1954. The main reason behind this is the difficulties to exploit these properties due to the cost and scarcity of large natural diamonds, and the fact that diamond was only available in the form of stones or grit. To overcome these problems, researchers realized that in order to form diamond, conditions are needed where diamond is in a more stable phase. The chemical vapor deposition (CVD) of diamond is one of the most popular, technically well understood and established, as well as commercially viable methods for synthesizing diamond. The first reproducible synthesis of artificial diamond, using a process requiring high temperature and high pressure was reported by General Electric Company in 1955 [1]. CVD was then used for the first time for synthesizing diamond by Eversole in 1962 [2].

CVD is a process in which gaseous precursors are introduced into a reactor and a solid is deposited on a usually hot substrate due to chemical reactions between the precursors. CVD is an atomistic process, in that the coat grows molecule by molecule. The consequence is that the process is slow and coatings are thin, but the result is a dense high quality deposit with good adhesion to the substrate due to atomic bond formation. Conventionally, the substrate is thermally activated to initiate the CVD reaction, typically above 800 °C. This could also be a serious limitation to some less stable sub-

strates. Alternative activation techniques have recently become available which can effectively lower the reaction threshold temperature to ~100 °C. These are laser-assisted CVD (LCVD), plasma-activated CVD (PACVD) and electron beam induced CVD (EBCVD). All CVD techniques for producing diamond films require a means of activating gas-phase carbon-containing precursor molecules. This generally involves thermal (e.g. hot filament) or plasma (DC or RF) activation, or use of a combustion flame (oxyacetylene or plasma torches). While each method differs in detail, they all share features in common. A detailed study on CVD diamond process and films is already done by Railkar et al. [3].

CVD diamond has properties that are very similar to those of natural diamond and yet it can be made in the form of large freestanding sheets that is extremely important for electronic applications such as substrates and heat spreaders. Beside such passive devices, CVD diamond has numerous attractive physical and electrical properties for active device applications, especially RF power electronics. The wide band gap, small (or negative) electron affinity, high breakdown voltage, high saturation drift velocity, high carrier mobility, radiation hardness and high thermal conductivity make diamond a promising material for fabrication of high power, high frequency and high temperature solid-state microelectronic devices, sensors/MEMS and vacuum microelectronic devices (e.g. field emission devices). The exceptional material properties of diamond is summarized in Table 1. A large number of research

Table 1  
Some exceptional properties of diamond

Property	Value	Comparison
Mechanical hardness (GPa)	80–100	SiC:40
Thermal conductivity (W/cm K)	5–20	Ag:4.3, Cu:4.0, BeO:2.2
Fracture toughness (Mpa/vm)	5.5	SiO <sub>2</sub> :1, SiC:4
Young's modulus (GPa)	1050	SiC:440, Graphite:9
Coefficient of thermal expansion (ppm/K)	1.2	SiO <sub>2</sub> :0.5
Refractive index	2.41@590 nm	Glass: 1.4–1.8
Transmissivity	225 nm–far IR	–
Coefficient of friction	0.05–0.1 (in air)	Teflon:0.05
Band gap (eV)	5.4	Si:1.1, GaAs:1.43
Electrical resistivity (Ωcm)	10 <sup>12</sup> –10 <sup>16</sup>	AlN:10 <sup>14</sup>
Density (gm/cm <sup>3</sup> )	3.51	Si:2.32, Cu:8.89

groups and manufacturers all over the world are currently working on different applications relevant to diamond [4].

From RF applications perspective, our study first demonstrates the material issues and technological challenges related to diamond; then we examine the potentials of diamond under these technological challenges, discover the key features of each device type or application and illustrate the simulation results based on our survey for comparison with theoretical aspects. We finally discuss the current status and expectations as well as future trends of diamond-based RF device technology.

## 2. Material issues and technological challenges

The field of ordered and disordered carbon covers a wide range of materials and properties from the soft, black and electrically conductive graphite to the extremely hard, bright and lustrous diamond, which is a near perfect insulator. This wide range of properties and various forms of carbon arise due to the different bonding configurations of the carbon atom. In principle a carbon atom can adopt any of three different bonding configurations,  $sp^3$ ,  $sp^2$  and  $sp^1$ . The bonds in the  $sp^3$  orbital are called ‘saturated’ bonds and others are ( $sp^2$  and  $sp^1$ ) ‘unsaturated’. Saturated bonds lead to lend strength to the bonds and therefore lead a more stable structure. This structure has a band gap of about 5.5 eV and is commonly known as diamond. The reason for such a large band gap is that p-states of diamond can penetrate into the region occupied by the 1s-state. Therefore they are closer to the nucleus and experience a stronger attractive potential from the nucleus. The diamond structure has a face-centered cubic (FCC) lattice with two atoms per lattice. Almost all physical properties of diamond are dependent on its crystal structure. Single crystal diamond shows the maximum values for all properties, which then falls off as one moves from polycrystalline to microcrystalline and finally to amorphous forms of carbon. For example, the hole mobility at room temperature for homoepitaxial CVD diamond film is about 1470  $cm^2/Vs$ . In comparison it is 229  $cm^2/Vs$  in the highly oriented diamond film and 70  $cm^2/Vs$  in the polycrystalline films [3].

The electronic properties of CVD diamond is examined by Nebel et al. [5]. In large grain CVD diamond they approach the properties of single crystal Ib or IIa diamond. In small grain CVD diamond the optical and electronic properties are governed by amorphous carbon-like density of states present at grain boundaries. Therefore, the properties are widely spread: The dark conductivity at a high temperature is activated with energies between 1 and 1.7 eV. The activation energy decreases significantly towards lower temperatures. From

charge collection experiments it is concluded that nominally undoped CVD diamond is an n-type semiconductor. The mobility of holes and electrons in CVD diamond can be as high as in natural or HPHT synthetic diamond but generally  $\mu_e$  and  $\mu_h$  are significantly smaller in PCD and HOD due to energy barriers at grain boundaries. The typical drift length measured by charge collection experiments is in the range of the grain size. The sub-band gap absorption of poly-CVD diamond is well described by an amorphous graphite density of state distribution present at grain boundaries. EPR experiments detect carbon defects (H1) at grain boundaries and nitrogen (P1) in the range of  $10^{17}$ – $10^{18} cm^{-3}$ , which is the origin of the n-type character of CVD diamond. Finally, spectrally resolved photocurrents show very different properties compared to optical absorption measurements. The onset of photocurrent is around 1 eV, increasing several orders of magnitude towards a shoulder in the range 2–3 eV. Only in high quality PCD layers are the PC characteristics comparable to Ib single crystalline diamond. As photo-generated electrons and holes are separated by trapping in grains (holes) and in grain boundaries (electrons), a persistent photocurrent effect is generated in these films. If progress in heteroepitaxial growth of single crystal CVD diamond continues, it is reasonable to assume that the electronic properties of CVD diamond will approach those of single crystal natural or HPHT synthetic diamond.

Williams et al. has shown that ‘black’ diamond, usually associated with passive applications such as thermal management due to its perceived low quality, performs as well as ‘high quality’ white polycrystalline diamond when hydrogenated to generate p-type characteristics. The performance is also similar to results reported by others for single-crystal diamond. This important observation may considerably improve future prospects for diamond-based active electronic devices due to the dramatic reduction in substrate cost that the use of black diamond would lead to [6].

To date there has been only limited success in producing n-type regions in diamond or p-type regions in SiC, while n-type doping of SiC by nitrogen implantation and p-type doping of diamond with boron are well-established processes. One way around this problem is to combine these two materials in order to exploit this complementary behavior for fabricating p–n heterojunctions or n-type regions in insulating diamond, and preliminary experiments have shown that ion-beam synthesis could be a suitable way to produce SiC diamond heterostructures in microscopic regions. Heera et al. reported two ways of achieving these heterostructures; diamond formation by high-dose carbon implantation in crystalline SiC, and SiC formation by high-dose silicon implantation in natural diamond [7]. The Diamond Group at Walter Schottky Institute, Germany is currently

Table 2  
Comparison of different poly-C deposition methods

Method	HFCVD	MPCVD	DC Arc-Jet CVD
Deposition rate ( $\mu\text{m/h}$ )	0.1–10	0.1–10	30–150
Substrate temperature ( $^{\circ}\text{C}$ )	300–1000	300–1200	800–1100
Deposition area ( $\text{cm}^2$ )	5–900	5–100	<2
Advantages	Simple, large area	Quality, stability	Quality, high rate
Disadvantages	Contaminations fragile filament	Rate	Contaminations small area

investigating AlGaN/diamond heterojunctions. A successful attempt to combine p-type diamond with n-type AlGaN to obtain a heterojunction bipolar p–n diode has recently been presented [8].

The synthesis of diamond at low pressures by CVD techniques is of interest both for its crystal growth science and as a process with significant commercial potential. The low pressure CVD approach is the only realistic alternative to high temperature-high pressure (HTHP) synthesis methods. Although diamond films have been synthesized in the laboratory by a number of methods, our discussions are limited mainly on three most commonly used techniques employed mostly by commercial vendors and research groups around the world [9,10]. These are DC Arc-Jet discharge, hot filament and microwave plasma enhanced CVD techniques. A comparison of these methods is given in Table 2.

One important issue for characterizing CVD diamond films comes with forming ohmic and Schottky contacts. An ideal ohmic contact is considered as one that does not add significant parasitic impedance to the structure and does not sufficiently change the equilibrium carrier concentration within the semiconductor or affect the device characteristics. Gerbi et al. investigated the contact behavior of various metals on n-type nitrogen-doped ultrananocrystalline diamond (UNCD) thin films [11]. Near-ideal ohmic contacts are formed in every case, while Schottky barrier contacts prove more elusive. Looi et al. have also studied characterization of diamond ohmic and Schottky contacts [12]. For “p-type surface” conductive diamond films, which rely on a H-terminated surface, Au forms ohmic contacts and Al near-ideal Schottky contacts. A detailed work about the electrical properties of Al-Schottky contacts on Hydrogen-terminated diamond is also presented by Garrido et al. [13]. Nearly any diamond electronic or sensor device needs at least one ohmic contact. These contacts play a key role in the overall device performance. Werner reviewed the dependence of the Schottky barrier height on the surface termination and the impact of annealing of carbide-forming metals on the specific contact resistivity to diamond [14]. It is concluded that carbide patches dominate the specific contact resistivity after annealing. Furthermore, the doping dependence of the specific contact resistivity and suitable diffusion barriers, which avoid interdiffusion of the contact scheme, are briefly discussed. The ohmic or rectifying contact

behaviour depends very much on the surface termination. From an industrial point of view, oxygen-terminated surfaces with reproducible properties are most easy to achieve. The contact resistivity depends strongly on the doping level concentration. In the p-type diamond, doping levels much larger than  $10^{20} \text{ cm}^{-3}$  can be easily achieved, therefore ohmic contacts to p-type diamond are simple. Furthermore, contact annealing of carbide-forming metals leads to the formation of carbides at the metal–diamond interfaces. This reduces the contact resistivity further. Contact resistivities as low as  $10^{-7} \Omega\text{cm}^2$  can be achieved after annealing. It was shown that the carbide is not necessarily a complete layer but can consist of carbide patches with a small diameter. These patches (most likely with a lower barrier height) have a significant impact on the specific contact resistivity. It can be expected that the size and density of the carbide patches will depend on the reactivity of carbide forming metal, annealing temperature and number of crystal defects on the surface. However, good ohmic contacts to the n-type diamond are not so well understood. The carbide formation does not have the same effect compared with the p-type material. The reported contact resistivities are extremely high ( $>10^3 \Omega\text{cm}^2$ ) and are not useful for practical applications. Furthermore, diffusion barriers, either for surviving the annealing step or for high temperature applications, have to be improved. Polycrystalline metals that include Pt or Pd are not a proper choice. In contrast, amorphous diffusion barriers look much more promising.

Perhaps the most challenging side of diamond RF semiconductor device design is the understanding and controlling the heteroepitaxial growth of diamond. Synthesis and processing challenges can be mainly categorized into three groups; substrate, doping and surface. Processing challenges begin with the substrate since diamond does not possess a natural substrate. In the past, all attempts to grow diamond single crystal quasi-substrates on a foreign base resulted in polycrystalline layers, well suited for MicroElectroMechanical Systems (MEMS) but not electronic devices. Up to now state-of-the-art results for diamond electronic devices were obtained on high temperature high pressure (HTHP) synthetic single crystalline stones. Although this will not allow wafer scale device manufacturing, the stones are already of chip size and their use may still be an attractive approach to demonstrate a discrete high

power diamond device [15]. Only recently there have been encouraging results concerning diamond growth on Iridium, obtaining a single crystalline quasi-substrate for electronic devices. Another serious hurdle is doping, the most important pre-requisite for electronic devices. Boron is the only deep acceptor which partially activated at room temperature. n-Type doping by nitrogen or phosphorous is (up to now) not effective enough to produce high electron densities and its use in transistor structures is very restricted. Therefore, bipolar junction transistors are out of the question, even though the principal mode of operation has been demonstrated [16,17]. However, the activation energy of boron decreases with increasing doping concentration and becomes negligible for net concentrations of  $N_A \geq 10^{20} \text{ cm}^{-3}$ . Therefore it is possible to fabricate boron doped layers with full carrier activation and a low temperature dependence of their conductivity.

Despite these limitations/technical challenges, electronic devices like MESFETs, MISFETs and even BJTs have still been presented using the surface conductivity property of CVD grown diamond film. Since the sheet charge in the conduction channels of electronic devices needs to be limited, nanometer-range channels called “ $\delta$ -channels” are needed which require monolayer doping and growth control. On the other hand, the hydrogen terminated surface induces a thin p-type conductive surface channel, which also features all characteristics of a ‘ $\delta$ -channel’ and which is RT activated, however without using extrinsic doping. The surface of these channels is a crucial part of the devices structures (such as field effect transistor (FET) structures), where the gate cannot be buried. In diamond, understanding the surface properties is especially important in conjunction with the p-type surface conductive channel found on the highly polar hydrogen terminated diamond surface. The channel is a two-dimensional hole gas (2DHG) [18], although the exact location of this channel (on or below the surface) and the nature the acceptor still remain under discussion.

Besides synthesis and processing challenges; quality of films, thermal characterization post synthesis processing as well as integration, cost and yield are the main issues to be improved when considering diamond as an RF power device. Nevertheless, the theoretical performance of diamond leads one to exceptional Figure of Merit (FOM) values when compared to any semiconductor material. Due to unique material properties, diamond shows the best theoretical performance for any Figure of Merit definition. Since discussed in detail by Ozpineci et al. [19], we will briefly summarize some theoretical aspects for comparison with other technologies:

- $f_{\text{max}}$  is theoretically 53 times better than Si for n-type diamond (42 times in p-type);

- Maximum breakdown voltage of a diamond power device is 514 times higher than Si (This is 56 for 6H-SiC, 46 for 4H-SiC and 34 for GaN);
- Thermal conductivity; diamond leads other materials by at least a factor of five;
- The Figure of Merit values, defined for high temperature, power and frequency operations of devices, for diamond are at least 40–50 times more than any other semiconductor.

### 3. Diamond RF electronics

The unique material properties leading to extreme FOM values and hence an extraordinary theoretical performance makes diamond attractive for RF electronics applications. Although the research is still at the device level which means in its early stage some promising results have already been obtained and even some diamond devices (SAW and FE devices) have been commercialized. The status of diamond based RF electronics which includes diodes, BJT, FET, MEMS, SAW and FE devices is discussed in detail in this part.

#### 3.1. Diamond based diodes

Schottky rectifiers have been used in many applications due to being majority carrier devices, providing fast switching time and no reverse recovery current. They also have lower forward voltage drop, appropriate when a low forward voltage in on-state is required. In recent years, significant progresses have been made on diamond-based Schottky diodes. Gildenblat et al. has reported high temperature Schottky diode with thin film diamond [20]. The reported diodes exhibited rectifying  $I$ - $V$  characteristics in the range of 26–500 °C. Ebert et al. reported high current p/p<sup>+</sup>-diamond Schottky diode with a low series resistance of 14  $\Omega$  at 150 °C and of 8 at 500 °C [21]. The circular contact area of these devices were  $5 \times 10^{-5}$  to  $10^{-3} \text{ cm}^2$  and the boron doping concentration were  $1.1 \times 10^{17} \text{ cm}^{-3}$ . A diamond Schottky diode with operation temperature up to 1000 °C has also been reported [22]. The barrier heights of Al and Au rectifying contacts on p-diamond were reported by Hicks et al. [23]. Stults reported that the current conduction mechanism of the diamond-based MIS diode structure is dominated by space charge conduction mechanism and also found that Ni, Al and Au form Schottky contacts on as-grown diamond film [24].

Despite a steady progress, there is still a large gap between theoretical and practical performance of the diamond-based Schottky diodes. The high-voltage and high-temperature performances of these diodes have been limited by material defects and the stability of the metal-diamond interface. In order to stay competitive

with the other WBS for high power/temperature applications, the leakage currents need to be reduced and the breakdown voltage must be improved. For further breakthroughs to achieve these goals, there are four critical issues to be resolved with epitaxially grown diamond films: growth and doping processes, structural design and selection of metal for Schottky contact. A diamond-based diode can be achieved in three forms; a metal-diamond Schottky diode, a Metal-Insulator Diamond (MIS) diode and a p–n diamond diode.

Diamond diodes have been fabricated in synthetic and natural single crystal diamond substrates and polycrystalline diamond layers grown on silicon or other non-diamond substrates. A simple, straightforward, diamond-based diode can be achieved in the form of a metal-diamond Schottky contact [25]. Unfortunately, the high cost of fabrication and dopant problem is still a barrier for practical applications but successful attempts are presented using CVD diamond films. Schottky diodes on oxygen-terminated surfaces show good performance at high temperatures, i.e. acceptable forward currents and high breakdown voltages at reverse bias. [26–28]. Fig. 1 shows the planar structure of the device, with 0.5  $\mu\text{m}$  i-diamond inserted between metal and doped-diamond, and its  $I$ – $V$  characteristics at room temperature. Although polycrystalline diamond Schottky diodes have been shown to have the highest voltage breakdown of 500 V of any published Schottky diodes, based on heteroepitaxy grown diamond films, the diodes have large forward resistances. The same structure, with only utilizing 0.25  $\mu\text{m}$  thick i-diamond, provided a forward current density of  $\sim 100 \text{ A/cm}^2$  [28]. Thus far, this is one of the highest current density reported with the heteroepitaxially grown PDF-based diodes on silicon substrate. This large resistance is the result of poor ohmic contacts, non-optimum device geometry and hydrogen electrically compensated boron impurities. Some of these devices have contact system

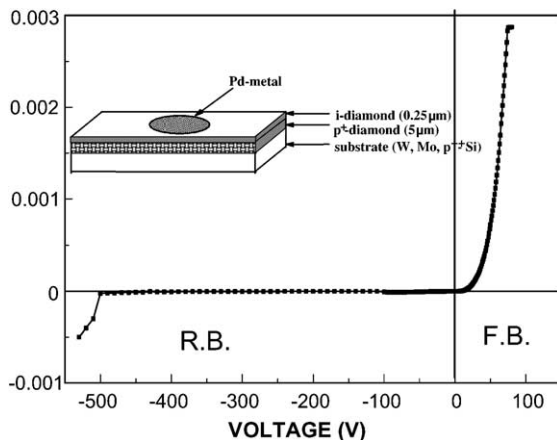


Fig. 1.  $I$ – $V$  characteristics of planar, metal (Pd)-intrinsic diamond-semiconductor diamond (MIS) diode at room temperature.

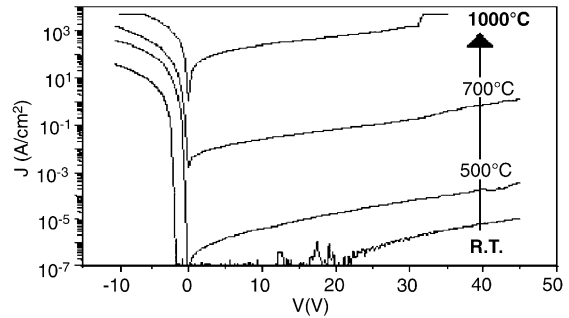


Fig. 2. Operation of diamond Schottky diode from RT to 1000 °C.

that has several layers and diodes using this contact metal stack have operated up to 1000 °C as seen in Fig. 2 [26]. Under optimum conditions the calculated forward resistance using uncompensated boron doped diamond [28] is between 0.01 and 0.1  $\Omega\text{cm}^{-2}$  for diodes with a breakdown voltage of 10 kV. Similar diodes formed in Si would have a resistance of 30  $\Omega\text{cm}^{-2}$ . The breakdown voltage of a diode depends upon the fundamental properties of the semiconductor and the minimum controllable doping density, which is limited by growth technology. Fig. 3 compares the breakdown voltage of diamond, SiC and Si as a function of doping. Note that its breakdown voltage is higher than SiC and Si at the same doping level.

Williams et al., reports the formation of thin overlayers on relatively inexpensive contaminated ‘black’ polycrystalline diamond grown by hot-filament chemical vapor deposition [29]. Effective Schottky diodes have been produced by this technique but are still far from ideal. These devices could be improved further by modifying the device structure. A microboron-doped diamond Schottky emitter for microelectronic sources is recently presented [30]. The fabricated diamond emitter shows high brightness emission current of 800 nA at a tip-anode (screen) electric field of 0.55 V/ $\mu\text{m}$  and tip heating voltage of 25 V. From the estimation using the Schottky emission model, the temperature of the emitter

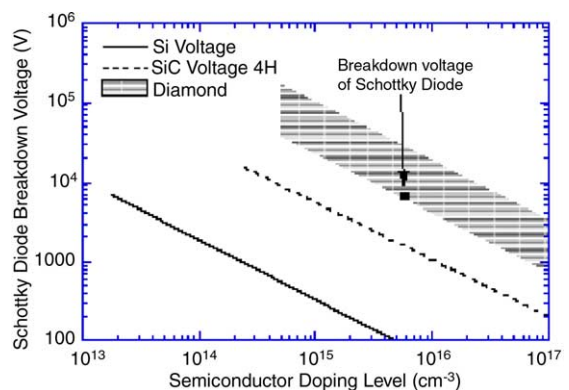


Fig. 3. Breakdown voltages of diamond, SiC and Si as a function of doping.

was found out  $862 \pm 10$  °C. Suzuki et al. have fabricated lateral dot-and-plane (with ring-shaped-gap) Schottky barrier diodes [31]. Frequency-dependent capacitance measurements revealed the existence of a deep donor level.  $C-V$  measurements deduced that the net donor concentration was  $6.2 \times 10^{17} \text{ cm}^{-3}$  and the corresponding built-in potential was 4.0 eV, when the P concentration was  $8.3 \times 10^{17} \text{ cm}^{-3}$ . Another application area of diamond Schottky diodes is chemical gas sensors. A study on Schottky diode based gas sensors is recently published for detecting  $\text{O}_2$ ,  $\text{H}_2$ ,  $\text{CO}$ , and hydrocarbons like benzene ( $\text{C}_6\text{H}_6$ ) and toluene ( $\text{C}_7\text{H}_8$ ) gases [32–34]. It is shown that a large sensitivity, fast response, high selectivity, wide dynamic range, repeatable/reproducible response for these chemicals can be obtained with diamond-based gas sensors, also very candidate for harsh environment applications.

Microwave Plasma CVD allows polycrystalline diamond to be grown on many different substrates and more practically than homoepitaxial diamond films. Despite the grain boundaries and defects in polycrystalline diamond films, MIS diodes have been demonstrated [35]. The metal-schottky junction usually suffers from large leakage current for practical diode applications. To reduce the leakage current, the effects of putting an insulating layer between the metal and the polycrystalline diamond (PCD) have been examined. The use of the MIS contacts has thus far been one of the best ways to both improve the breakdown voltage and reduce the leakage current of PCD diodes [36]. The structure of a MIS diode is shown in Fig. 4.

Despite the difficulty in forming n-type diamond, the first diamond p–n junction diode was reported in the early 1990s [37]. The semiconducting diamond layers were deposited using hot filament CVD with  $\text{P}_2\text{O}_5$  and  $\text{B}_2\text{O}_3$  as the n- and p-dopants, respectively. The pn-junction properties were studied by the temperature-dependent analysis of the forward and reverse current characteristics ( $I-V$ ) and by RT capacitance–voltage ( $C-V$ ) measurements [38,39]. The  $I-V$  characteristics of a pn-junction diode are shown in Fig. 5. The curves in

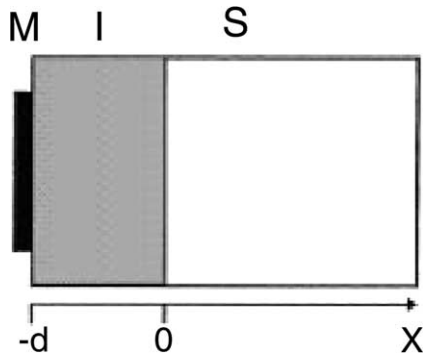


Fig. 4. MIS diode structure.

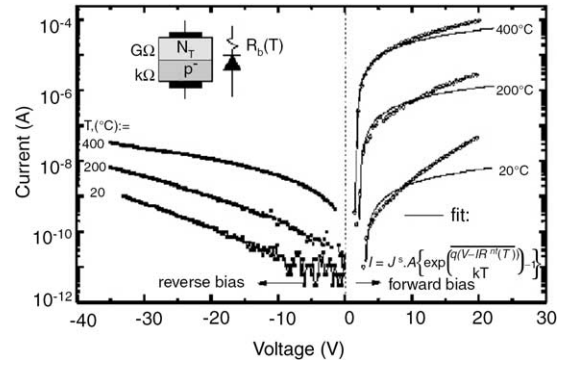


Fig. 5.  $I-V$  characteristics of a diamond nitrogen/boron pn-junction diode.

Fig. 5 show that in the forward direction the diode can be fitted with the analytical model for a pn-junction with a temperature-dependent series resistance.

### 3.2. Diamond BJT

Prins reported the first diamond BJT in 1982 on natural, p-type single crystal diamond [16]. The n-type conducting layer was made by carbon implementation into the p-type single crystal diamond. The primitive device had a low-current amplification factor of 0.11. The absence of a reliable shallow donor remains the bottleneck of diamond bipolar devices like bipolar junction transistor (BJT). For that reason, little attention has been paid to their development except for a single publication in 1982 about bipolar diamond transistor by ion implantation. Aleksov et al. presented the first analysis of this kind of device by using a pnp BJT structure with nitrogen-doped base. For this purpose both p–n diodes and  $p^+ np$  bipolar junction transistor structures were fabricated by MPCVD growth using nitrogen and boron for the first time [40]. The device features a nitrogen-doped base  $\sim 200$  nm thick, as seen in Fig. 6.

The analysis of pn-diodes show that high series resistance of the semi-insulating base will limit BJT operation. The  $G\Omega$ -range of the base series resistance,  $R_B$ , provokes high input voltages in order to lower the

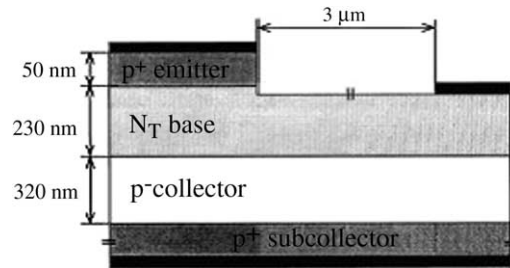


Fig. 6. Cross-Section of a diamond pnp BJT structure with n-type base using deep nitrogen donor.

emitter-base junction potential. This induces leakage currents in the reverse biased base-collector junction. Therefore transistor action could only be observed in the nA-current range. The DC current gain in common-base configuration was measured approximately 200. In the common-emitter configuration this value was measured to about 3, mainly because of the higher-base collector reverse bias that causes a higher leakage current across the junction. Due to the temperature activation of leakage current transistor operation was only observed up to 200 °C. Studies on junctions between boron- and nitrogen-doped diamond layers show that despite its deep activation energy level the fabrication of abrupt pn-junctions with a high built-in voltage is feasible [41,42]. Sumitomo fabricated pn-junctions and the BJTs on heavily boron-doped HTHP single crystals. The junctions were fabricated entirely from epitaxially grown layers.

Recently, diamond bipolar electron devices have made steady progress in meeting the expectations set by the ideal material properties; however, they perform still well below estimated limits. Thus, the devices presented need to be experimented more for further development. This is especially the case with bipolar transistors (BJTs) using boron/nitrogen pn-junctions since the nitrogen donor level has activation energy of 1.7 eV and nitrogen-doped layers, therefore, represent a lossy dielectric with high sheet resistance.

### 3.3. Diamond FETs

Due to the ideal diamond materials properties field effect transistors (FETs) in diamond should theoretically outperform FET structures on other wide band gap materials like SiC and GaN in high power RF applications. However, the difficulties in the technology of these structures results in two device concepts investigated by Aleksov et al. [26];

- Boron  $\delta$ -doped channel FETs:
  - (i) Boron  $\delta$ -doped channel MESFET
  - (ii) Boron  $\delta$ -doped channel JFET
- Surface channel FETs:
  - (i) Surface channel MISFET
  - (ii) Surface channel MESFET

#### 3.3.1. Boron $\delta$ -doped channel FETs

In FETs the channel carrier density is that of the ionized impurities, whereas the channel depletion will depend both on ionized and non-ionized impurities [43]. In consequence, a channel with deep impurities will yield low currents due to incomplete ionization, but at the same time the electrical field strength necessary to deplete the channel will be the same as in the case of full activation. In diamond full activation of the boron

acceptor at RT is obtained only for doping concentrations  $N_A \geq 10^{20} \text{ cm}^{-3}$ . In this case, the sheet charge and therefore the thickness of the channel are limited by the breakdown field thus leading to  $\delta$ -doped channels representing a challenge for diamond epitaxy, since precise growth of a monolayer is necessary.

With respect to  $\delta$ -channel-FETs, the  $\delta$ -channel-MESFET with a Schottky-gate have been investigated [44,45]. The original doped channel MESFET concept suffered from incomplete carrier activation and has therefore not been continued after the basic modes of FET operation had been demonstrated. In contrast, the  $\delta$ -channel-FET approach contains an extremely narrow window for the  $\delta$ -doping profile. At a peak concentration of  $10^{20} \text{ cm}^{-3}$  the boron doping spike needs to be confined to only a few nanometer to contain a limited sheet charge, which can still be depleted within the materials breakdown field of  $10^7 \text{ V/cm}$  for diamond (three times that of GaN). Therefore, initially a tool to refine the  $\delta$ -profile was needed. This was the adjustment of the channel sheet charge by differential etching while monitoring the channel current. Then, the gate needed to be placed on the rear side (back gate approach) of the channel by means of a pn-junction. Since only nitrogen was available for n-type doping (with an activation energy of 1.7 eV), the gate resistance was extremely high and the gate represented a lossy dielectric, restricting operation to quasi-DC.

The potential advantages of diamond pn-junctions in diamond  $\delta$ -FET structures over Schottky contacts are a low leakage current and high breakdown as well as the higher built-in voltage of above 3.0 V compared to the 1.7 V of the Schottky contact. This leads to a shift in the pinch-off voltage towards enhancement-mode operation. In the JFET the gate metal is separated from the channel by an N-doped layer as shown in Fig. 7. The n-doped layer is a lossy dielectric represented by a leakage resistor in parallel to the dielectric capacitance inserted in between the gate metal and channel. Depending on the layer properties and dimensions the behavior can be either resistive or capacitive.

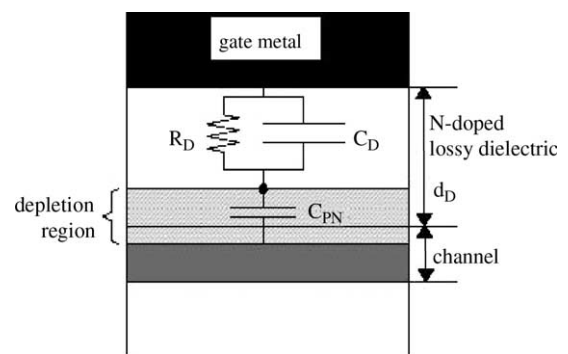


Fig. 7. N-doped lossy dielectric layer between gate metal and channel of a diamond JFET.



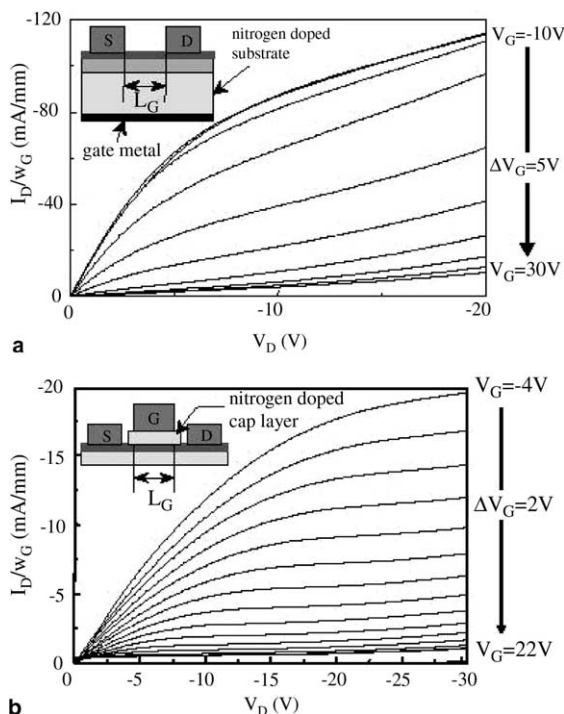


Fig. 8. DC characteristics of (a) back-gate JFET at 250 °C; (b) top-gate JFET at 200 °C.

There are two possibilities to place the gate control junction; on top as conventionally done or at the channel backside [44,45]. Fig. 8a and b demonstrates these structures and their  $I-V$  curves [26].

### 3.3.2. Surface channel FETs

In surface channel FETs, a p-type surface channel induced by hydrogen termination of the surface is used. This channel in fact is a 2DHG following closely the surface topography. This up to now prevents the implementation of a gate recess and therefore all structures of this type are planar. Kawarada pioneered the basic structure [46]. Today two different structures with two different gate configurations are pursued: the surface-channel-MESFET [47,48] and the surface-channel-MISFET [49,50]. Although the physical/chemical nature of this channel configuration is still under discussion, this type of FET structure is the only one to have demonstrated cut-off frequencies in the Gigahertz range.

Surface-channel-MISFETs have been developed using SiO and CaF<sub>2</sub> as a gate dielectric [49]. Most promising results have been obtained using CaF<sub>2</sub> avoiding any oxygen contamination, which might disturb the hydrogen-terminated surface. Such MISFET structures have been realized with sub-micron gate length and sub-micron gate to source and drain contact spacings and have therefore yielded in high extrinsic current gain cut-off frequencies for a gate length of 0.7 μm. The maximum transconductance of 100 mS/mm was obtained by DC measurement. The cut-off frequency of 11 GHz and

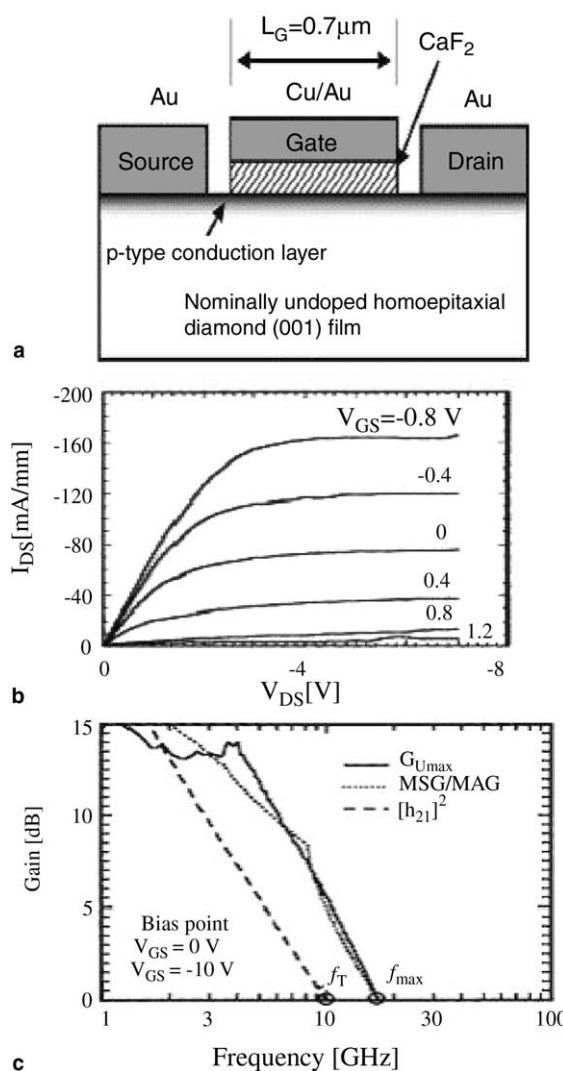


Fig. 9. (a) Cross-section of a 0.7 μm gate-length diamond MISFET; (b)  $I-V$  curves of a 0.7 μm gate-length diamond MISFET; (c) characteristic frequencies of a 0.7 μm gate-length diamond MISFET.

the maximum frequency of oscillation of 18 GHz were achieved for the fabricated MISFET [50]. The cross-section,  $I-V$  curves and characteristic frequencies of the MISFET above are given in Fig. 9.

A recent study of deep sub-micron surface-channel MISFETs is done by Matsudaira et al. [51]. The sub-micron gate (0.23–0.5 μm) diamond MISFETs were fabricated on an H-terminated diamond surface. Basic characteristics of the FETs are investigated for the high-frequency performance of the diamond MISFETs. The short channel effect is well suppressed utilizing thin gate insulator compared with the gate length. The transconductance increases as the gate length reduces down to 0.2 μm. Maximum transconductance of 71 mS/mm in DC mode and of 51 mS/mm in AC mode was obtained. The  $f_T$  of 40 GHz is expected to be realized in 0.25-μm gate MISFET without parasitic resistance.

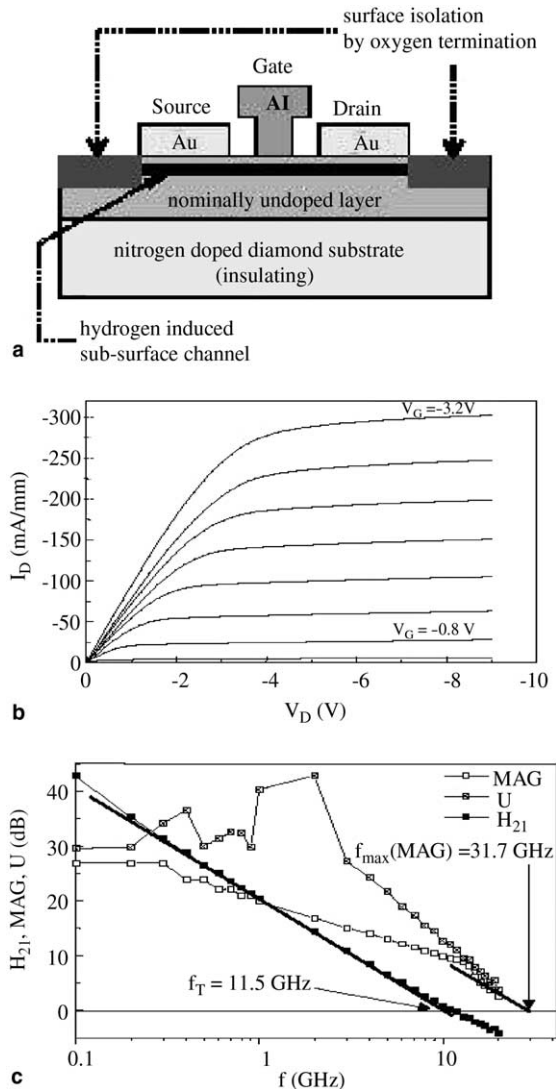


Fig. 10. (a) Cross-section of a 0.2  $\mu\text{m}$  gate-length surface-channel-MESFET; (b)  $I$ - $V$  curves of a 0.2  $\mu\text{m}$  gate-length surface-channel-MESFET; (c) characteristic frequencies of a 0.2  $\mu\text{m}$  gate-length surface channel MESFET.

Hydrogen-induced surface conductive channels are very attractive for the fabrication of diamond MESFET devices. Surface p-type channel devices show extremely low leakage current and high breakdown voltages. The most successful MESFET approach uses self-aligned gate technologies by etch back of the Au-ohmic contact metallization through the resist window for gate metallization, shown in Fig. 10a. In this way 0.2- $\mu\text{m}$  gate length devices with high  $f_{\text{max}}/f_T$  ratios could be realized. Fig. 10b shows the DC-output characteristics of such a surface-channel-MESFET with 0.2  $\mu\text{m}$  gate length fabricated by standard T-gate e-beam lithography as used for InP and GaAs HEMTs [52]. Maximum drain current reaches above 300  $\text{mA mm}^{-1}$  and the maximum drain bias up to 68 V giving a possible RF output power of up to 3  $\text{W mm}^{-1}$ . However, the RF tests of this device

were limited to small signal parameter measurements at low drain current due to unstable performance at high current levels. The cut-off frequencies  $f_T$  and  $f_{\text{max}}$  were extracted from the current gain plots as shown in Fig. 10c. Here  $f_{\text{max}}$  was extracted from both the maximum available gain plot  $f_{\text{max}}(\text{MAG})$  and the maximum unilateral gain  $f_{\text{max}}(\text{U})$ . The maximum values obtained were  $f_T = 11.5$  GHz and  $f_{\text{max}}(\text{MAG}) = 31.7$  GHz and  $f_{\text{max}}(\text{U}) = 40.22$  GHz. The high  $f_{\text{max}}/f_T$  ratio of above 3 is related to the high voltage gain of above 100 obtained from the  $g_m/g_{\text{DS}}$  ratio. This high  $f_{\text{max}}$  values enables the millimeter-wave operation but DC measurements were not accomplished due to instability problems caused by the surface.

Diamond field-effect transistors (FETs) with their channel partially oxidized and highly resistive can also be fabricated by ozone treatment [53]. These FETs are operated in electrolyte solutions. It is shown that from X-ray photoelectron spectroscopic (XPS) analyses, it is evident that hydrogen-terminated (H-terminated) diamond is partially oxygen-terminated (O-terminated) by ozone treatment. The quantification of surface oxygen shows that the surface oxygen increases with an increase in ozone treatment time indicating the control of oxygen coverage. The partially O-terminated diamond surface channel is much less conductive compared with the H-terminated diamond. The ozone-treated FETs were operated stably even though the channel of the FETs becomes highly resistive. The sheet resistance increases with ozone treatment time, however, the sheet carrier density decreases with the ozone treatment time. For the sensing of particular ions or molecules by the immobilization of sensing components, the control of surface termination is necessary. Upon comparing the  $I$ - $V$  characteristics of the non-treated FET with the ozone-treated FET, the threshold voltage of the FET is shifted in the negative direction by the ozone treatment. It is considered that the decrease of surface band bending (the increase in electrical resistivity) on the diamond surface by partial oxidation includes this threshold shift phenomenon. As the reason for this, such as the difference in electron negativity between the H-terminated and O-terminated surfaces is considered. Consequently, in the ozone-treated FET, more gate bias is needed to achieve the same level of hole accumulation as in the non-treated FET.

Looi et al. have suggested Hydrogen doped thin film diamond FETs for high power applications [54]. Thin film polycrystalline diamond Schottky diodes and MESFETs have been produced which display unprecedented performance levels. The primary origin of the improvement achieved is the use of near surface hydrogen to produce p-type diamond as opposed to the incorporation of boron. The processes, which enable hydrogen to create p-type characteristics, appear to be almost fully activated at room temperature and device structures

with stable characteristics can be fabricated and operated at temperatures as high as 200 °C. This enables to make realistic predictions for the power handling capabilities of this form of device. Modest scaling of the simple devices would lead to a MESFET structure capable of operation at 0.2 W/mm (with a  $V_{DS}$  value of 100 V); optimized structures may operate at powers as high as 20 W/mm, which is considerably greater than state-of-the-art SiC devices.

Nippon Telegraph and Telephone Corp. (NTT) have developed a diamond semiconductor device that operates at 81 GHz, more than twice the speed of earlier devices [55]. The advance promises to make amplification in the millimeter-wave band from 30 to 300 GHz possible for the first time. The NTT lab has been in collaboration with the University of Ulm in Germany, which had already succeeded in fabricating FET devices, to develop a diamond semiconductor device using its diamond thin-film layer. The joint team formed T-shaped gates on the diamond layer, which is on a 3-mm<sup>2</sup>-diamond substrate. The gate width, which determines the performance of devices, is 0.2 micron. NTT is now working to further decrease impurities to improve the quality of diamond crystal. It is targeting devices with an operating frequency of 200 GHz and an output power of 30 W/mm.

### 3.4. Diamond RF MEMS

The unique combination of material properties of diamond, such as piezoresistivity, mechanical hardness, low coefficient friction and high thermal conductivity makes it ideal for applications such as physical sensors and MEMS. Piezoresistivity is a particularly useful effect for realizing a diamond physical sensor. Moreover, the wide band gap of diamond indicates that the piezoresistive effect is “hard”, that means, it is preserved or even accentuated at higher temperatures and in radiation environments that severely limits present materials [56]. These properties and the ability to fabricate polycrystalline diamond films with semiconductor processing indicate diamond may provide advanced sensors and actuators for MEMS applications operating at high temperature–high pressure in harsh environments where Si and GaAs cannot perform.

The design of RF circuits is based on a common reference impedance of 50 Ω for interconnects and wiring. However, power devices may deviate essentially from this value in their output and input impedance. Thus, transistor structures are usually surrounded by passive matching networks acting as impedance transformers. Other passive components are filters and switches in TR (transmit and receive) modules or antennas. All these passive components need to be placed on insulating substrates to avoid losses. Therefore, materials used are insulators like quartz, sapphire or various plastics. In monolithic

integration the semiconductor needs to be semi-insulating which brings a problem with using Si (even when being high resistive), and MEMS technologies for passive components try to use air gaps for isolation. Diamond on the other hand can be an ideal insulator with low losses even at millimeter-wave frequencies [57].

Mechanical RF filters of high Q are generally realized with freestanding beam resonators [58]. The mechanical resonance frequency is a function of the materials Young’s modulus. It may be seen that due to its extremely high Young’s modulus diamond resonators may be possible in the Gigahertz range using sub-micron structures. The highest resonance frequency measured to date is 640 MHz [59] and has been obtained with double-anchored cantilevers using a thin nano-diamond film of high quality.

Electrical switches are an essential part of many electronic systems reaching from switching of microwave power in radar systems and low loss switches in high resolution measurement systems to fuses and circuit breakers. Thus, they may represent a high volume market, which in turn may enable further development of a material ultimately capable to be used in electronics. This would open up the perspective for ultra high power high temperature electronic systems. A classical electrostatically driven cantilever beam structure switch is sketched in Fig. 11 [60]. All essential parts of the switch (base plate driving contact, anchor, cantilever beam and contacts) are made of diamond. The support of the base plate is a silicon wafer.

Schmid et al. investigated microswitches based on polycrystalline diamond films [61]. Device properties such as switch-on and switch-off times are calculated and compared to measurement results obtained from fabricated structures. They calculate the influence of various geometric parameters on the transient behaviour of the switches. It is shown that diamond improves the transient behaviour of the devices in comparison with other materials such as silicon. The results indicate that for operation in air a diamond microswitch exhibits an approximately eight times higher maximum frequency of operation than a silicon microswitch of identical geometry.

The potential of diamond RF MEMS is recently reviewed by the Diamond group in University of Ulm,

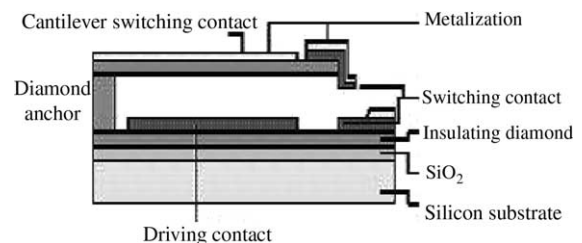


Fig. 11. Schematic cross-section of diamond electrostatic microswitch.

Germany [62]. They are concentrated on the development of diamond microwave switches in a coplanar arrangement. The advantage in using diamond not only as base plate material is manifold as for example: diamond contacts avoid sticking, the large stiffness of the beam allows high switching speed and the high thermal conductivity allows high power switching. Two driving concepts have been evaluated. Firstly, it is the conventional electrostatic drive, operating by capacitive force. It has no DC loss. The disadvantages of this concept are high driving voltages and low contact force. Alternatively, the bi-metal effect has been employed in an electrothermal driving concept. In this concept the cantilever is bent by thermally induced stress. The actuation voltage can be as low as 1.3 V. However, thermal power is applied to close the switch and is also needed to keep it closed. To circumvent this severe disadvantage a bi-stable switching configuration, based on a prestressed double-anchored beam has been evaluated [63–65].

It seems at this early stage in their development that the most promising area for future development will be in the field of microelectromechanical structures where their friction, stiction and wear properties make them prime candidates for use in moving mechanical assemblies. As a consequence, diamond is an attractive base for RF MEMS; furthermore it is also attractive to develop all diamond structures based on membranes and freestanding beam structures. Nevertheless the picture is not complete with the few examples mentioned.

### 3.5. Diamond-based surface acoustic wave (SAW) devices

One of the most attractive applications of diamond is a surface acoustic wave (SAW) device, for diamond has the highest sound velocity among all materials. Recent progress in CVD technology of diamond has made it possible to develop SAW devices using diamond film, and a great deal of progress has been made in the research and development of this device [66].

Diamond has the highest acoustic velocity among all materials due to its high Young's modulus, and thus its SAW velocity is also the highest. And so, it will be of good use to high-frequency SAW devices providing great advantages in the manufacture and durability of the device. For example, a 5 GHz SAW filter has been fabricated with the electrode of 0.5  $\mu\text{m}$  width with the diamond SAW, whereas electrodes less than 0.2  $\mu\text{m}$  are necessary for the conventional SAW materials [67]. Besides the highest Young's modulus, diamond also has the highest thermal conductivity. This will also provide the advantage for high power handling of SAW devices.

Fig. 12 shows a schematic diagram of a diamond SAW filter. Since diamond does not have piezoelectric-

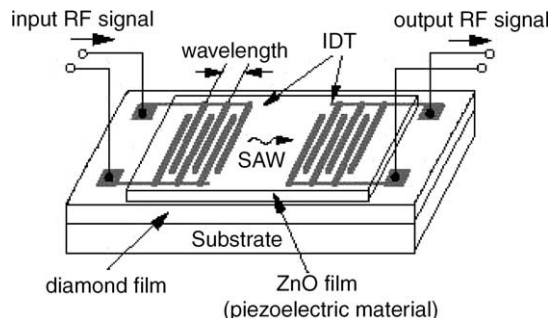


Fig. 12. Schematic diagram of a diamond SAW filter.

ity, it must be combined with a piezoelectric layer such as a ZnO film for the generation of the SAW. The smoothness of the substrate surface is the significant requirement for the SAW applications because the rough surface will lead to a large propagation loss of the SAW energy, and the surface polishing of the diamond film is another key technology. Propagation loss, high power durability and effect of velocity dispersion are other challenges of diamond SAW devices [68].

Among the variety of applications of diamond, the SAW filter is the first commercial product as an electronic device using diamond. Some companies (such as Sumitomo in Japan) are already exploiting diamond-based SAW filters in commercial mobile phone equipment, and it is likely a diamond SAW filter to be an essential component of all high frequency communications equipment, including telephone networks, cable television and the Internet.

### 3.6. Diamond field emission devices

Field emitter arrays (FEAs) are very attracting electron sources in a wide variety of applications, including microwave power amplifiers (MPA), field emission displays, and electron microscopy. One of the most attracting features of FEA emitters is that the nature of their emission process, direct density modulation of the electron beam at RF frequencies becomes possible. This implies that there is extremely low electron transit time and high transconductance in triode structure with grid gate, making it possible to lift an upper modulation frequency to more than 2 GHz.

Milne et al. describes the PECVD growth of vertically aligned arrays of carbon nanotubes, which are suitable for use as the electron emitters in a novel type of microwave amplifier capable of producing of order 10 W at 30 GHz [69]. These field emission devices are vacuum tubes and should not be confused with the solid-state power devices. The application area will be the long-range telecommunication systems that are based upon microwave links. The transmitters use helix traveling wave tubes (TWTs) which in the very near future will be required to work at up to 30–100 GHz with output power in the region

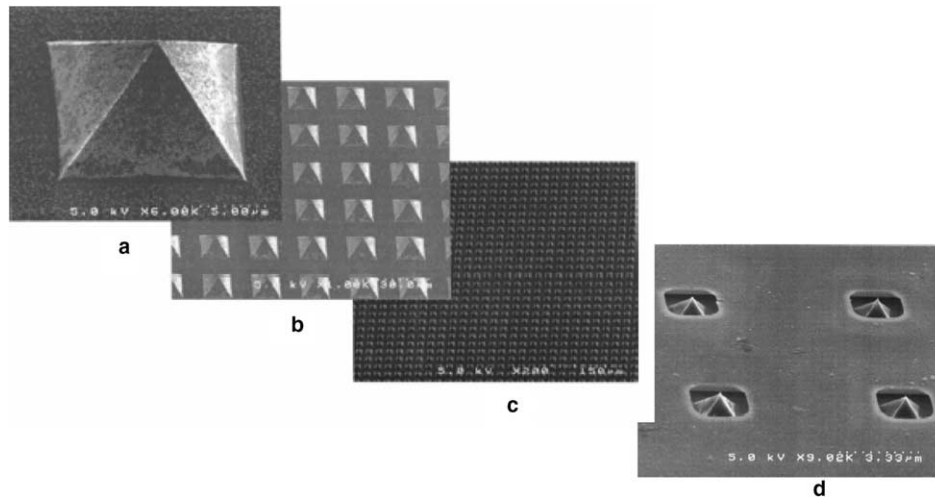


Fig. 13. SEM of a portion of a large array of diamond microtips with  $12\ \mu\text{m}$  base-width and  $10\ \mu\text{m}$  base-base spacing between adjacent tips: (a) detailed geometrical dimensions of a single diamond microtip at high magnification; (b, c) low magnifications of diamond tips demonstrating good uniformity among tips; (d) SEM picture of the gated/triode diamond field emission triode device.

of 5–10 W. Spindt et al. reported the performance of the fabricated the annular molybdenum (Mo) FEA, which was treated by in situ hydrogen plasma cleaning, for microwave applications [70]. Whaley et al. also reported the FEA-TWT using a 1-mm diameter Mo emitter with a custom designed electron gun and helix circuit. They demonstrated that the FEA-TWT has operated with a maximum current of 91.4 mA and shows 99.5% transmission under both drive and no-drive conditions [71]. However, a conventional fabrication process of FEA needs expensive and complicated semiconductor technologies. For comparison, at the present time photomixers with low temperature-grown GaAs can provide a power of 1 mW at 1 THz with a roll-off of 12 dB per octave at higher frequencies [72], but no wide-band tunable sources are available for higher frequencies. Simulations show that photomixing in resonant laser-assisted field emission can cause the emitted current to oscillate at frequencies from dc to over 100 THz, so this technique shows promise for new ultra wideband devices.

Kang and coworkers have also reported the development of vertical and lateral diamond field emission devices [73–78]. Vertically self-aligned gated diamond vacuum triodes were fabricated on a silicon-on-insulator (SOI) mold, as shown in Fig. 13. This fabrication flow utilizes conventional silicon micropatterning and etching techniques to define the anode, gate and cathode. The fabrication has achieved diamond field emitter triodes over practical wafer areas. Vertical diode structures show high cathode current potential. The field emission of the triode array exhibits transistor characteristics with high DC voltage gain (800) and good transconductance. Also, lateral diamond vacuum diodes were fabricated with a diamond patterning technique utilizing an oxide mask and lift-off. An anode–cathode spacing of less than

$2\ \mu\text{m}$  between the diamond anode and cathode was achieved. The lateral diode exhibits a low turn-on voltage of 5 V (field  $\approx 3\ \text{V}/\mu\text{m}$ ) and a high emission current of  $6\ \mu\text{A}$ , from four diamond cathode ‘fingers’ configuration, as presented in Fig. 14. The lateral diamond field emitter has potential applications in vacuum microelectronics, sensors and MEMS. Fig. 15 shows anode emission current vs anode voltage ( $I_a-V_a$ ) of a self-aligned gated diamond emitter triode with four tips in (a), anode emission current vs gate voltage ( $I_a-V_g$ ) of a self-aligned gated diamond emitter triode with four tips in (b), FN plot of a self-aligned gated diamond emitter triode in (c).

### 3.7. Thermal management with diamond devices

Modern high-power electronic and opto-electronic devices suffer severe cooling problems due to the production of large amounts of heat in a small area. In order to cool these devices, it is essential to spread the narrow heat flux by placing a layer of high thermal conductivity between the device and the cooling system (such as a radiator, fan, or heat sink). CVD diamond has a thermal conductivity that is far superior to copper over a wide temperature range plus it has the advantage of being an electrical insulator. Now that large-area CVD diamond plates with thermal conductivities  $\approx 20\ \text{W}/\text{cm K}$  are available [79].

Diamond heat spreaders were successfully bonded to device wafers of either silicon or GaAs using gold-tin eutectic solder with proper metallization procedures. AlN embedding layer improves the adhesion strength of diamond to molybdenum or silicon nitride, thermal stability of the bond and the heat spreader characteristics. Jagannadham has shown that multilayer diamond films exhibit higher effective thermal conductivity than either single layer diamond or molybdenum [80].

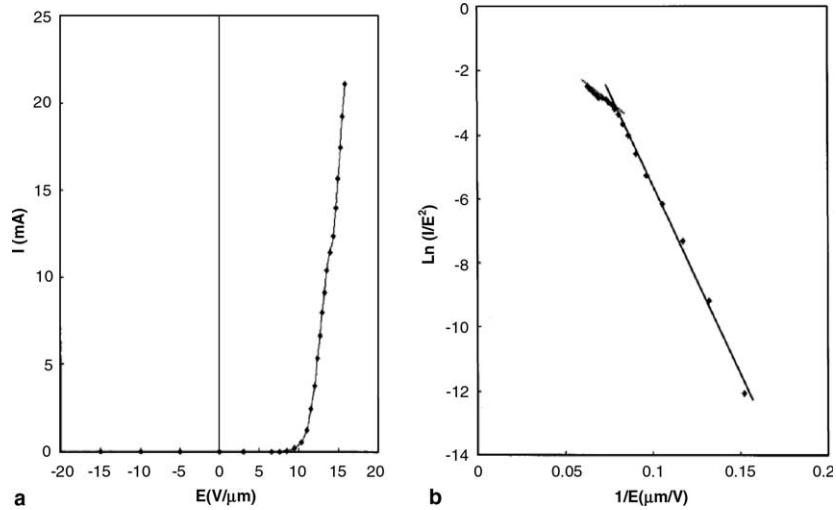


Fig. 14.  $I$ - $E$  plot of diamond vacuum diode with high emission current (a), F-N plot of diamond vacuum diode with high emission current (b).

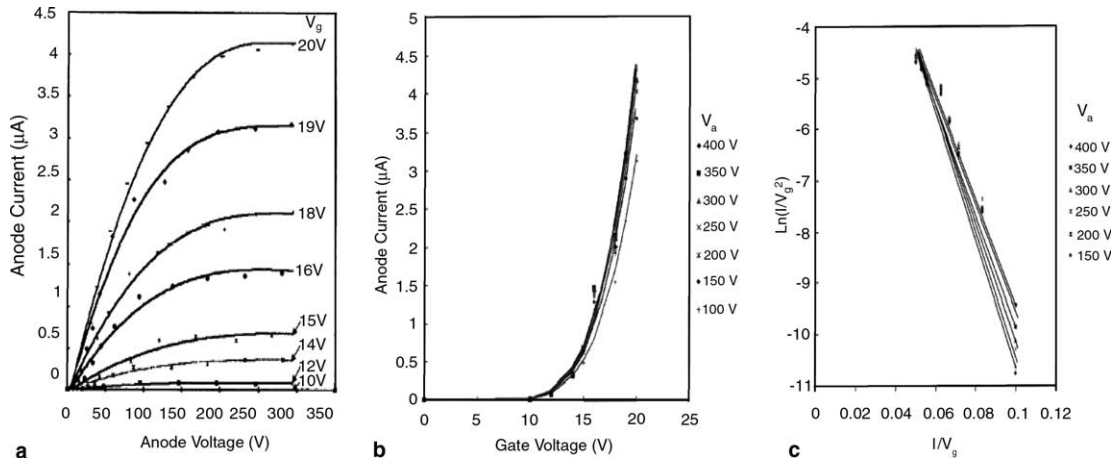


Fig. 15. Anode emission current vs anode voltage ( $I_a$ - $V_a$ ) of a self-aligned gated diamond emitter triode with four tips (a); anode emission current vs gate voltage ( $I_a$ - $V_g$ ) of a self-aligned gated diamond emitter triode with four tips (b); FN plot of a self-aligned gated diamond emitter triode (c).

Souverain et al. have studied the sensitivity of thermal resistance,  $R_{TH}$ , to parameters such as substrate thickness, its nature (GaAs, Si, AlN or diamond), the

topology of the power source (length and width), or even the power density and show that the transfer of active layers onto a host substrate with a higher conductivity such as Si, AlN or diamond is of greater interest than thinning of the substrate [81]. They have developed a thermal model for AlGaAs/GaAs heterojunction bipolar transistor (HBT) and have shown that if the HBT layers are transferred onto a diamond substrate, a 50% gain in RF power can be expected at 10 GHz. By this method, the reduction in static and mainly dynamic performance of the device due to the low thermal conductivity of GaAs can be improved. As shown in Fig. 16, at 10 GHz, an output power of 1W below 150 °C can be obtained with diamond host substrates where the same amount of power is attained at about 250 °C for the GaAs substrates. Besides the applications discussed above CVD diamond film technology can also

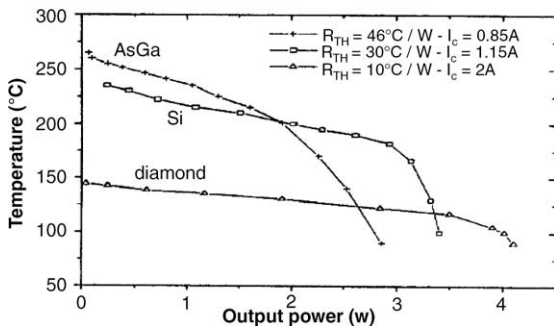


Fig. 16. HBT temperature vs. output power at 10 GHz.

be applied to chemical gas sensors [82,83], electroanalysis electrodes [84], particle detectors [85], cutting tools [86], radiation detection devices [87] and optics [9].

### 3.8. Performance summary of diamond RF devices

As it theoretically has the highest values for any FOM definition, diamond should outperform all other semiconductor materials. However, since diamond technology is in its infancy and relatively few experimental results are successful/obtained, there may rise many questions related to the suitability of diamond for a technology choice in RF applications. For comparison and performance evaluation, we give key features and some results obtained with each device type using diamond technology. Table 3 is a summary of these results and current status.

- Bipolar junction transistors (BJTs)
  - Deep doping problem
  - High resistivity of the Nitrogen doped base, (10 GΩcm at 20 °C)
  - nA current range
  - Operation temperature below 200 °C (leakage currents dominate)
  - Base transport is around 100 GHz due to high carrier mobility
  - With nitrogen doped base the only area will be high DC current gain applications
  - 50–70 GHz cut-off frequencies
  - For accurate modeling, high series resistance of the base, leakage of reverse bias p-NT junctions and surface leakage must be examined
  - Common base configuration;  $\beta$  is up to 200 where it is 1.1 in common emitter configuration
- Field effect transistors (FETs)
  - Maximum drain bias of 200V is demonstrated
  - Power density of nearly 30 W/mm is extracted (measured value is 0.35 W/mm at 1 GHz,  $L_G = 0.4 \mu\text{m}$  with 400 Ω load)
  - $f_T = 21 \text{ GHz}$  and  $f_{\text{max}} = 63 \text{ GHz}$  is measured (for 0.2 μm gate length)

- Passivation issues has not been addressed yet
- Most promising active devices
- Passive components and MEMS
  - RF filters of high  $Q$  with 640 MHz resonance frequency obtained
  - Diamond contacts avoid sticking
  - High power and high speed switching with diamond contacts
  - Coplanar waveguides have been realized
  - Elementary switching of MW signals in a coplanar waveguide arrangement has been demonstrated
  - Diamond RF MEMS and all diamond structures based on membranes and free standing beams are attractive
- Surface acoustic wave (SAW) devices
  - First commercial diamond electronics product
  - Promising for high frequency equipment
  - Likely to replace conventional SAW filters
- Field Emission (FE) devices
  - Oscillation from DC to 100 THz obtained
  - Promising for long range telecom systems

## 4. Summary and future trends

Despite some material difficulties such as the search for large area monocrystalline substrates and dopant problems, diamond can be seriously considered as a base material for RF electronics, especially RF power circuits. It is shown that diamond power devices will be capable to generate very high power levels at microwave frequencies. In addition many microdevices has been demonstrated on polycrystalline films. Up to now the development of these devices has made steady progress and many diamond electronic devices have already met important milestones in their development process. These milestones include pn-junction operation as well as the evaluation of diamond BJTs, However, this case is based only on the boron/nitrogen pn-junctions. Diamond Schottky diodes on both single and polycrystalline material have proven their extraordinary potential for high-temperature electronics. The most challenging devices both with respect to technology and perspective are diamond FETs, where simulations promise an extraordinary power handling capability.

The commercialization of diamond is still in its infancy despite the rapid progress made in the last decade in the science and technology behind diamond film CVD. Although simulations results are decent, there is still work remaining for the future to reach the figures of merit promised by the unique physical properties of diamond including substrate, doping and passivation problems as well as wafer costs. Researchers and industry are currently concentrating upon developing methods to scale up the CVD processes and reduce production costs. However, some devices are already

Table 3  
Performance summary of diamond RF devices

Device or application	Current status	Key feature	Key challenge
BJT	R&D	High DC $\beta$	Doping
FET	R&D	Most promising active device	Doping
MEMS	R&D	640 MHz resonance freq	Few examples
SAW devices	R&D, commercial	First commercial product	–
FE devices	R&D, commercial	100 THz oscillation freq	–

in the marketplace, such as diamond heat spreaders, windows, cutting tools, and SAW filters. In the next few years one can expect to see diamond films appearing in many more applications one and probably the most promising of which will be in the area of specialized flat-panel displays and high temperature electronics.

### Acknowledgements

This work was performed in the context of the network TARGET—“Top Amplifier Research Groups in a European Team” and supported by Information Society Technologies Program of the EU under contract IST-1-507893-NOE, [www.target-org.net](http://www.target-org.net).

### References

- [1] Bundy FP et al. *Nature (London)* 1955;176:51.
- [2] Eversole WG. US Patent No. 3030188, April, 1962.
- [3] Railkar TA et al. *Crit Rev Solid State Mater Sci* 2000;25(3):163–277.
- [4] <http://www.chm.bris.ac.uk/pt/diamond/>.
- [5] Nebel CE et al. *Semicond Sci Technol* 2003;12:S1–S11.
- [6] Williams OA et al. *Semicond Sci Technol* 2003;12:S77–80.
- [7] Heera V et al. *Appl Phys Lett* 2000;77(2):226.
- [8] Vogg G et al. *J Appl Phys* 2004;96(1):895.
- [9] Dischler B, Wild C, editors *Low-pressure synthetic diamond*. Springer; 1998.
- [10] May PW. *Phil Trans R Soc Lond A* 2000;358:473–95.
- [11] Gerbi et al. *Appl Phys Lett* 2003;83(10):2001–3.
- [12] Looi HJ et al. *Diam Relat Mater* 1999;8:966.
- [13] Garrido JA et al. *Appl Phys Lett* 2002;81(4):637.
- [14] Werner M. *Semicond Sci Technol* 2003;12:S41–6.
- [15] Aleksov A et al. *Diam Relat Mater* 2003;12:391–8.
- [16] Prins JF. *Appl Phys Lett* 1982;41:950.
- [17] Denisenko A et al. *Diam Relat Mater* 2000;9:1138.
- [18] Nebel CE et al. *Diam Relat Mater* 2002;11(3–6):351.
- [19] Ozpineci B, Tolbert LM. ORNL/TM-2003/257.
- [20] Gildenblat GS, Grot SA, Hatfield CW. *IEEE Electron Dev Lett* 1990;11:1811.
- [21] Ebert W et al. *IEEE Electron Dev Lett* 1994;15:289.
- [22] Vescan A et al. *IEEE Electron Dev Lett* 1997;18:556.
- [23] Hicks MC et al. *J Appl Phys* 1989;65:2139.
- [24] Stults T. MS Thesis 1994, Vanderbilt University, Nashville, TN, USA, 1994.
- [25] Kang WP et al. *J Appl Phys* 1995;78:1101.
- [26] Aleksov A et al. *Semicond Sci Technol* 2003;18(3):S59–66.
- [27] Butler JE et al. *Diam Relat Mater* 2003;12:S67–71.
- [28] Gurbuz Y et al. *IEEE Trans Power Electron* 2005;20(1):1–10.
- [29] Williams Oliver A et al. *Diam Relat Mater* 2002;11(March–June):396–9.
- [30] Bae JH. *J Vacuum Sci Technol B* 2004;22:1349.
- [31] Suzuki M et al. *Appl Phys Lett* 2004;84(March 29):2349–51.
- [32] Gurbuz Y et al. *Sensors Actuators B: Chem* 2004;99(1 May):207–15.
- [33] Gurbuz Y et al. *J Appl Phys* 1998;84(12):6935–6.
- [34] Gurbuz Y et al. *IEEE Trans Electron Dev* 1999;46:914–20.
- [35] Miyata K, Dreyfuss DL, Kobashi K. *Appl Phys Lett* 1992;60:480.
- [36] Huang Q-A et al. *Appl Surf Sci* 2001;171:57–62.
- [37] Okano K et al. *Solid-State Electron* 1991;34:139.
- [38] Kang WP et al. *J Electrochem Soc* 1994;141(8):2231–4.
- [39] Kubovic M et al. *Diam Relat Mater* 2004;13(April–August):802–7.
- [40] Aleksov A, Denisenko A, Kohn E. *Solid-State Electron* 2000;44:369–75.
- [41] Borst HT, Strobel S, Weis O. *Appl Phys Lett* 1995;67:2651.
- [42] Aleksov A, Denisenko A, Kohn E. *Proc Applied Diamond Conf Frontier of Carbon Technology Joint Conf 1999 (Tsukuba, Japan) 1999*. p. 138.
- [43] Ebert W et al. *Diam Relat Mater* 1997;6:329.
- [44] Shiomi H et al. *IEEE Electron Dev Lett* 1995;16:36.
- [45] Vescan A et al. *IEEE Electron Dev Lett* 1997;18(5):222.
- [46] Kawarada H. *Surf Sci Rep* 1996;26(7):205.
- [47] Aleksov A et al. *Diam Relat Mater* 2002;11:382.
- [48] Taniuchi H et al. *IEEE Electron Dev Lett* 2001;22(8):390.
- [49] Hokazono A et al. *Solid-State Electron* 1999;43:1465.
- [50] Ishizaka H. *Diam Relat Mater* 2002;11:378.
- [51] Matsudaira H et al. *Diam Relat Mater* 2003;12:1814–8.
- [52] Aleksov A et al. *Proc. 23rd (International Conference on Microelectronics) MIEL 2002*, vol. 1, Nis, Yugoslavia, 12–15 May, 2002.
- [53] Bassin C, Ballan H, Declercq M. *IEEE Electron Dev Lett* 2000;21(1):40.
- [54] Looi HJ et al. *Thin Solid Films* 1999;343–344(April):623–6.
- [55] Matsunaga K et al. *International Electron Devices Meeting IEDM 2000, San Francisco, CA, December 10–13, 2000*, Technical digest, paper 16.6.1.
- [56] Chatty K et al. *IEEE Electron Dev Lett* 2000;21(7):356.
- [57] Werner M. Piezoresistivity effect of boron doped diamond thin films, presented at the 3rd European Conf. on Diamond, Diamond-like and related coatings, Germany, Aug 31–Sept 4, 1992.
- [58] Thumm M. *Diam Relat Mater* 2001;10:1692.
- [59] Nguyen CT-C. *Vibrating RF MEMS for low power wireless communications, 2000 Int. MEMS Workshop (iMEMS'01), Singapore, (July 2001) Proceedings* 21.
- [60] Sekaric L et al. *Appl Phys Lett* 2002;81:4455.
- [61] Schmid P, Adamschik M, Kohn E. *Semicond Sci Technol* 2003;S72–6.
- [62] Aleksov A et al. *Diam Relat Mater* 2004;13:233–40.
- [63] Adamschik M et al. *Diam Relat Mater* 2002;11:672.
- [64] Ertl S et al. *Diam Relat Mater* 2000;9:970.
- [65] Schmid P et al. *Diam Relat Mater* 2003;12:418.
- [66] Milne WI. *Semicond Sci Technol* 2003;12:S81–5.
- [67] Nakahata H et al. *Semicond Sci Technol* 2003;18(3):S96–S104.
- [68] Wu T-T, Chen Y-Y. *Trans. on Ultrasonics, Ferroelectrics and Frequency control* 2002;49(1).
- [69] Milne WI et al. *Curr Appl Phys* 2004;4(5):513–7.
- [70] Spindt CA et al. *Vacuum Sci Technol* 1986;B14:1996.
- [71] Whaley DR et al. *IEEE Trans Plasma Sci* 2000;28:727.
- [72] Verghese S, McIntosh KA, Brown ER. *IEEE Trans Microwave Theory Technol* 1997;45:1301.
- [73] Wisitsora-at A et al. *J Vac Sci Technol B* 2003;21:1671.
- [74] Wisitsora-at A et al. *J Vac Sci Technol B* 2003;21:1665.
- [75] Wisitsora-at A et al. *J Vac Sci Technol B* 2003;21:614.
- [76] Wisitsora-at A et al. *Diam Relat Mater* 1999;8(July):1220–4.
- [77] Kang WP et al. *J Vac Sci Technol B* 2001;19:936.
- [78] Kang WP et al. *J Vac Sci Technol B* 1996;14:2068.
- [79] Worner E et al. *Diam Relat Mater* 1996;5:688.
- [80] Jagannadham K. *Solid-State Electron* 1998;42(12):2199–208.
- [81] Souverain P et al. *Microelectron Reliab* 1998;38(4):553–7.
- [82] Gurbuz Y et al. *Sensors Actuators B* 1999;56(1–2):151–4.
- [83] Kang WP et al. *Sensors Actuators B: Chem* 1995;25(1–3):421–5.
- [84] Martin H et al. *Diamond Films and Related Materials: 3rd Int. Conf. Washington, DC: NIST; 1995*. p. 91.
- [85] McKeag RD, Jackman RB. *Diam Relat Mater* 1998;7:513.
- [86] Reineck I et al. *Refract Metals Hard Mater* 1996;14:187.
- [87] Bergonzo P, Tromson D, Mer C. *Semicond Sci Technol* 2003;12:S105–12.